Joint Air-to-Surface Standoff Missile Baseline Aerodynamics

Tri Phan[1], Nathaniel Hollman[2], Tiger Sievers[3] and Mohamed Almazrouei[4],
University of Kansas, Lawrence, Kansas, 66045, United States

I. Executive Summary

This report discusses the aerodynamics of the JASSM missile, developed by Lockheed Martin. First, an operational range of speeds and altitudes were researched and postulated to develop the range of conditions the missile will experience. The missile was found to cruise at an altitude of 2,000-30,000 ft at Mach 0.71. There are two specified missions, one being launched from a crate suspended by a parachute, which starts the missile at a relatively low altitude and Mach number, and the other mission being launched from a high-speed, high-altitude fighter jet. A model of the atmosphere was developed, and the dynamic pressure ranges that the JASSM will experience were calculated. The body aerodynamic center of the missile then calculated and considered at different angle of attack, which is determined to be close to the nose in cruise flight and moving towards aft as angle of attack increases. The aerodynamics of the missile begin with the drag produced by the body, with the major contributions being from base and friction drag, due to the missile being subsonic. The normal forces from angle of attack were then calculated for the missile body, and the maximum lift to drag ratios were found. Because of the high aspect ratio of the wing and the subsonic cruising conditions, lifting surface theory was chosen to analyze the planar surfaces. Since the missile only experienced subsonic flight, drag due to friction was the only one analyzed. The tail size was determined to be zero, making the missile have a flying wing design. With that, the C.G. location could be determined to result in a tailless design.

[1] Responsible for Body Aerodynamic Center.
[2] Responsible for Standard Atmosphere, Body Geometry, and Body Drag.
[3] Responsible for Planar Surfaces and Aerodynamic Center, and Tail and Control Surface Sizing.
[4] Responsible for Cruise Flight Conditions and Body Normal Force.

II.Background

The Joint Air-to-Surface Standoff Missile (JASSM) is a stealthy, precision-guided cruise weapon designed to be launched from stand-off ranges, fly at low observable altitude, with terrain following profile to penetrate enemy air defenses, and deliver a high-explosive warhead onto a fixed target with guided terminal homing. In this design we retain the Lockheed Martin JASSM's baseline mission and guidance suite but replace the conventional horizontal tail surfaces with a streamlined boattail rear fuselage and optimized aft control fins if needed. The boattail reduces radar and aerodynamic drag while shifting stability and trim requirements rearward. This configuration aims to preserve low observable characteristics and range while trading some longitudinal stability for improved cruise efficiency and simpler external signatures.

Table 1 The JASSM Specifications

Baseline Design	Dimension
Body Diameter	21.61 in
Reference Area	369.25 in^2
Nose Length	40.68 in
Total Body Length	161.95 in
Elliptical Height	10.00 in
Elliptical Width	11.67 in
Roll Angles	0 deg
Nose-tip Diameter	0 in
Center of Gravity Assumption	0.5 total length
Effective Exhaust Area	23.76 in^2
Leading Edge Section Angles	0 deg
Number of Surfaces	3
Sweep Angles	45 deg
Wingspan	7.87 ft
Root Chord Length	1.00 ft
Nose Tip to Root Chord Leading Edge of Wing	60.6 in

Much of this geometry was found using a three-view of the JASSM rocket and using the total length as a base dimension [1]. The missile body was modeled in NX to measure the other derived geometry [2].

A. Mission Description

The JASSM can fly a variety of missions, including extremely different initial conditions. This report will observe these initial conditions and flight regime, specifically when discussing the dynamic pressure and Mach plots, as these conditions force the missile into vastly different circumstances. For both missions, the missile will aim to cruise at 2000 ft at 0.71 Mach to avoid radar detection to remain stealthy and will accelerate when descending to hit its target, reaching a speed of around Mach 0.9. The first mission is defined as being launched from a C-130, which

deploys a crate of the missiles that slowly descend to 10,000ft using a parachute. The JASSM is then deployed from the crate at this altitude, and once it reaches Mach 0.1 begins to have a controlled descent to 5,000 ft. The JASSM then begins powered flight to increase its Mach number from 0.3 to its cruising speed of Mach 0.71, and descends to 2,000 ft, where it executes the rest of the mission as usual. The other defined mission is the JASSM being launched at high altitude of 40,000 ft from a fighter jet at Mach 0.9. The theory behind this is that the fighter is in super cruise, possibly being an F-22, and slows to Mach 0.9 to launch the JASSM without forcing the missile into an unusual Mach range. The JASSM then coasts down to 30,000 ft with its wings deployed to save fuel and increase range and then begins powered flight while descending to 2,000 ft at Mach 0.71, where it will carry out the rest of its mission.

Operational Cruise Mach number: 0.71
Maximum Mach number: 0.9
Cruise altitude: 2000 ft – 30,000ft [3] and [4]
Operational AoA: less than 10 deg
Stall Effective AoA: 10 deg

III. Standard Atmosphere

The standard atmosphere was found using an online resource which provided the ratios of temperature, pressure, and density for increasing altitudes in kilometers [5]. A function was then created to interpolate this data, which was previously extracted to a .mat file for code efficiency. Atmospheric data was found for up to 80,000 feet in altitude, and the ratios of pressure, temperature, density, and the speed of sound are shown in Figure . Note that this data is the temperature states static values, or the stream values if observed at zero velocity.

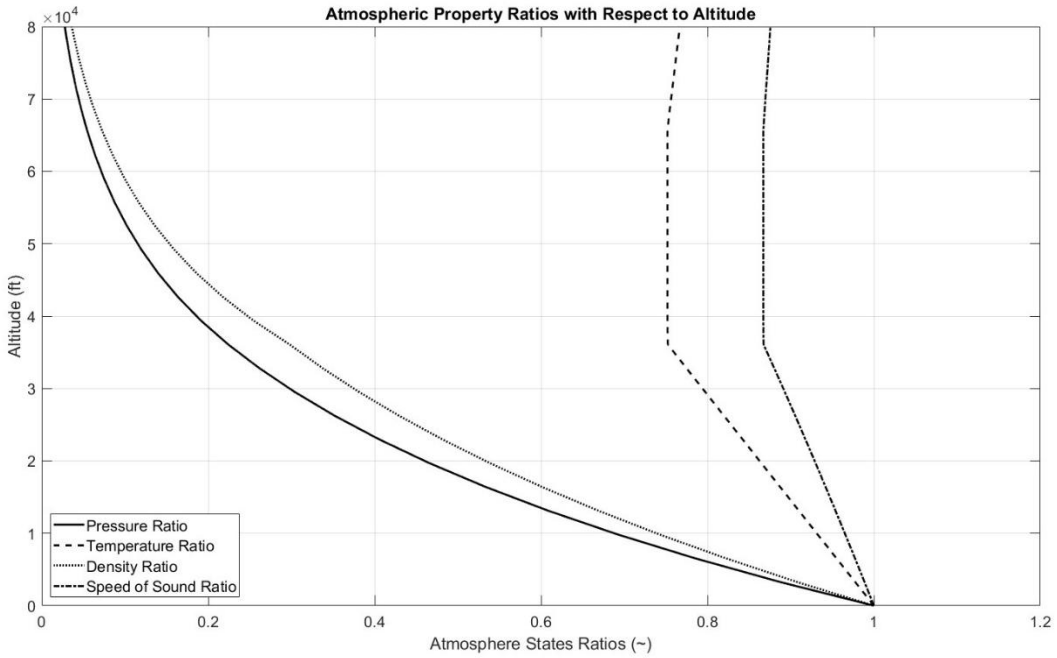

Figure 1 Standard Atmospheric State Ratios for 80,000 ft

These ratios are a multiplier of the local sea level absolute states. The standard sea level states were researched and found to be pressure = 14.7 psi, temperature = 518.7˚R, density = 0.002377 lb/ft^3, and the speed of sound = 1,117 ft/s. In general, pressure and density decrease with altitude and approach zero as they reach the boundary of space. Temperature decreases until around 40,000 ft, where it stays constant until around 65,000 ft where it starts increasing due to less protection from the sun. It was assumed for this that the gas constants did not change with altitude, so the speed of sound ratio varied to the square root of the temperature. While this is an inaccurate assumption, for our true operational altitude, these values will minimally change, meaning that the assumption is not inaccurate for our operational ranges. With a defined ceiling of 40,000 ft, the plot of the states can be narrowed to the operational range in Figure 2.

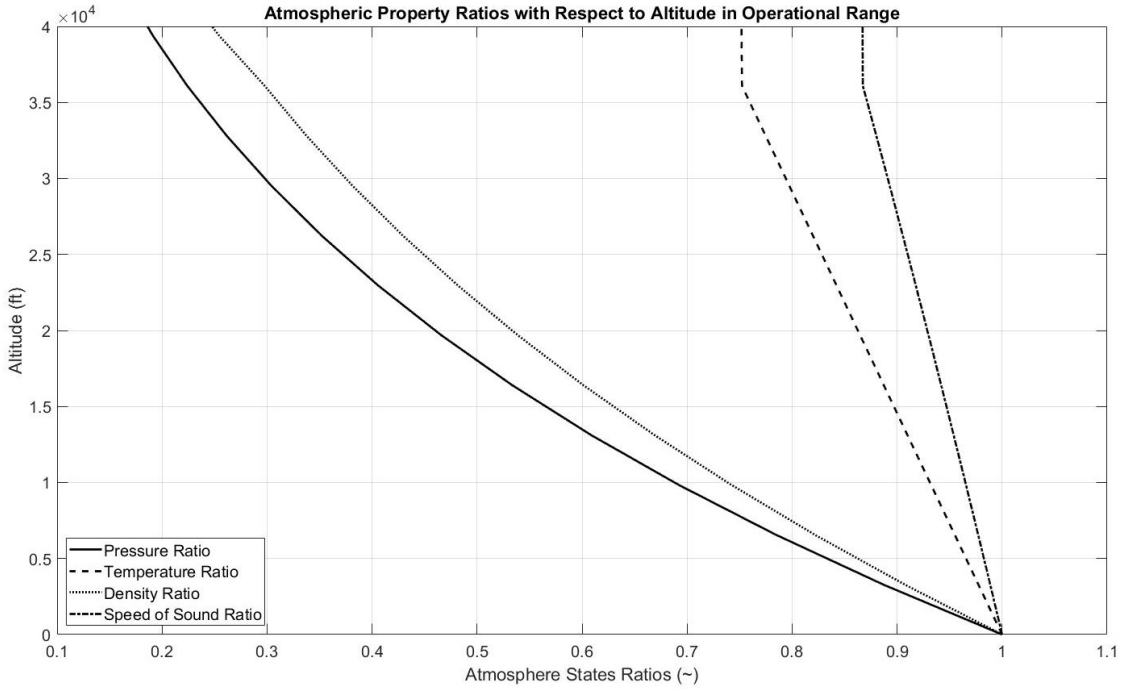

Figure 2 Standard Atmospheric State Ratios for Operational Range

The speed of sound ratio was then used to find the average Mach value for the operational range, which was found by averaging the ratio of the speed of sound and multiplying it by the ground speed of sound velocity. This yielded an average speed of sound of 1037 ft/s. The dynamic pressure can then be calculated for the operational range of Mach numbers using this average speed of sound and the change in density through altitude. The contours for these are shown for a range of Mach numbers in Figure .

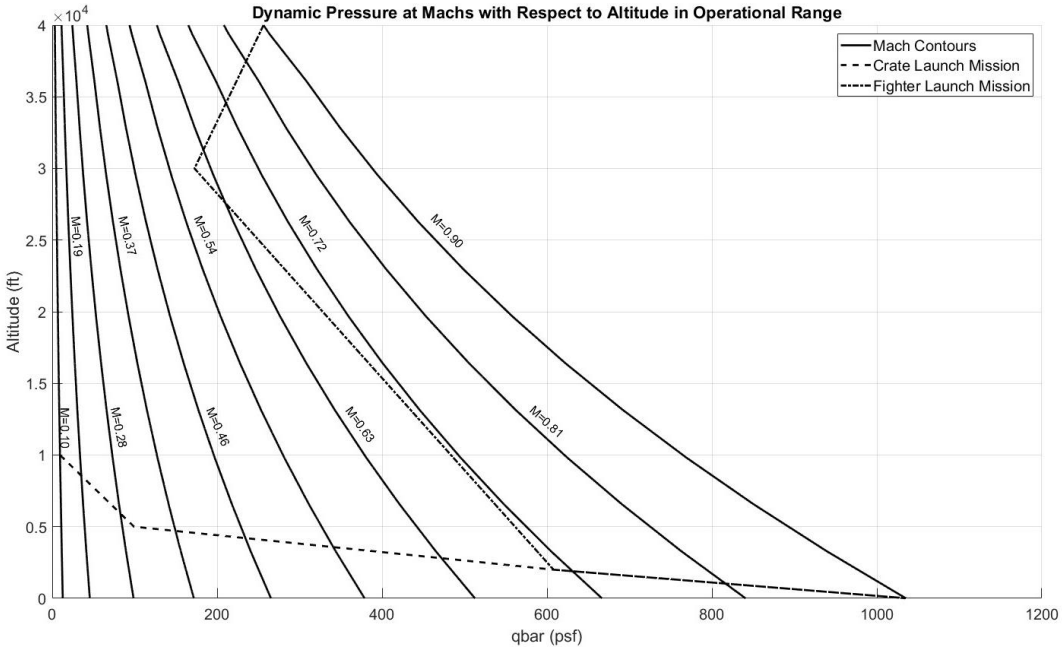

Figure 3 Dynamic Pressures at Various Mach Numbers and Altitudes

This plot also shows the two previously described missions flown in terms of altitude and dynamic pressure. Note that for different missions, the JASSM must be within a dramatically different range of dynamic pressures as its altitude and Mach speed vary significantly. This shows how the controller for the JASSM must consistently adapt to its current conditions, and the aircraft itself must be robust enough to fly at these varieties of conditions. As previously mentioned, in mission 1 the JASSM is launched at slow speed at low altitude from a parachute-suspended crate and descends to the cruise altitude of 2,000 ft at Mach 0.71. Mission 2 is when the JASSM is launched from a high altitude at a fast speed, such as from an F-22 at 40,000 ft, where it coasts to a lower speed, and then cruises to its point of Mach 7.1 at 2,000 ft. After this, it is estimated that on its descent to its target, it could reach a speed of Mach 0.9, so this is done to demonstrate the farthest extent of the dynamic pressure that the JASSM could experience. This entire range describes how the JASSM must be able to have a powerful enough control surface to maneuver at low dynamic pressures, while having an accurate enough surface to make minute adjustments at high dynamic pressures.

IV. Missile Body

The JASSM is equipped with a faceted and a flat window dome technology to provide low radar cross section and low dome error slope. The window dome has the advantage of low optical distortion for an IR seeker and low RCS. On the contrary, it limits the field of regard of the seeker, which may limit the ability of the seeker to acquire an off-boresight target. A faceted dome has the advantage of low electromagnetic and optical distortion because of the flat surfaces. In the other hand, the disadvantage of a faceted dome for an infrared seeker is the solar energy reflection off the facets into the seeker. The JASSM has a single window dome, the seeker has a limited field of regard and is biased downward to look through the window [6].

A. Body Drag

The total zero-lift drag coefficient of a body is the combination of skin friction drag, base drag, and wave drag. The drag is assumed to mainly be a function of speed and the missile geometry, and not a function of the angle of attack, so the drag is equal to the zero angle of attack drag. The contributions towards total C_{D0} are shown in Equation (1).

$$(C_{D_0})_{Body} = (C_{D_0})_{Body,Friction} + (C_{D_0})_{Base} + (C_{D_0})_{Body,Wave} \quad (1)$$

The major contributors of drag for a subsonic missile are friction and base drag. Wave drag is considered to be zero for the purposes of this missile, as any amount of wave drag when the missile is near Mach 0.9 is only applied for small amounts of time, and is thus a negligible amount of energy loss compared to the cruise segments. Base drag occurs when air flow separates from the body of the missile at the end of the missile. Base drag is lower for missiles with tapered ends, called boattails. The exhaust from the missile also decreases the base drag as the flow from the engine replaces the possible separated flow of the outside flow, increasing the pressure behind the body and thus decreasing drag. The equation for powered base drag and coast or unpowered base drag are shown in Equation (2) and Equation (3) respectively.

$$(C_D)_{Base,Powered} = \left(1 - \frac{A_e}{S_{ref}}\right)(0.12 + 0.13M^2) \quad (2)$$

$$(C_D)_{Base,Coast} = 0.12 + 0.13M^2 \quad (3)$$

The body friction drag is found using the dynamic pressure, length and diameter, and the Mach number, and is shown in Equation (4).

$$(C_D)_{Body,Friction} = 0.053\left(\frac{l}{d}\right)\left[\frac{M}{ql}\right]^{0.2} \quad (4)$$

The total coast and powered body drag coefficient is then generated in Figure 4.

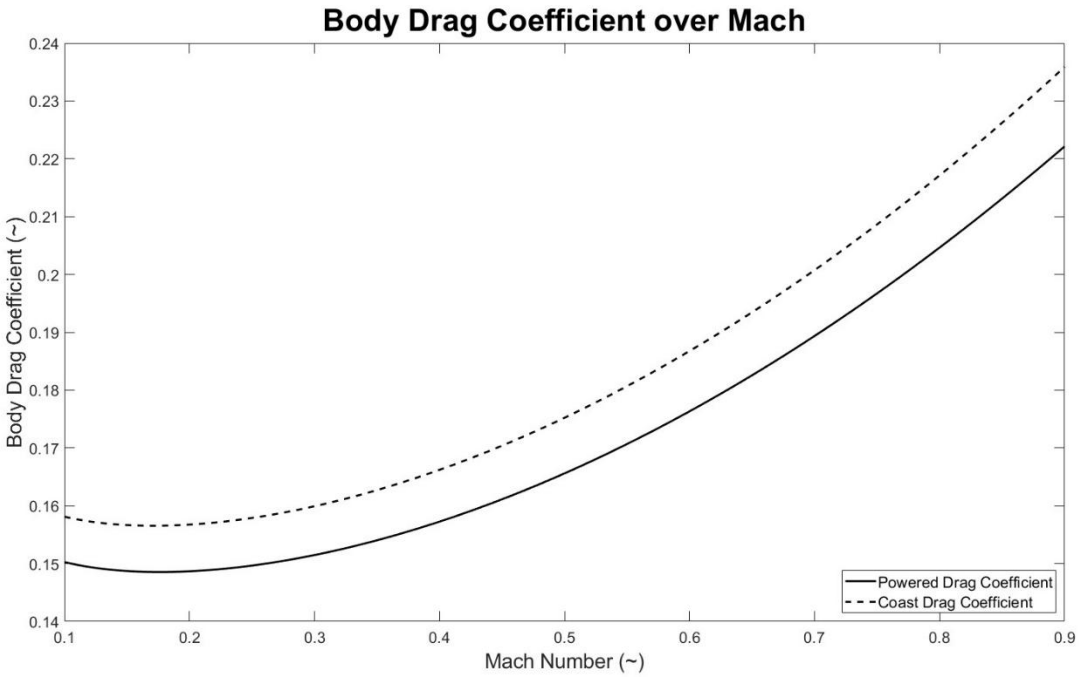

Figure 4 Total Drag Coefficient for Mach Range

As shown in Figure 5, the base drag coefficient is not constant, it increases with Mach number throughout the subsonic range. As the JASSM's speed increases, the pressure in the wake behind the base tends to decrease further, amplifying the pressure difference and increasing the base drag coefficient. The skin friction drag is also a weak function of the Mach number, dynamic pressure, and body length.

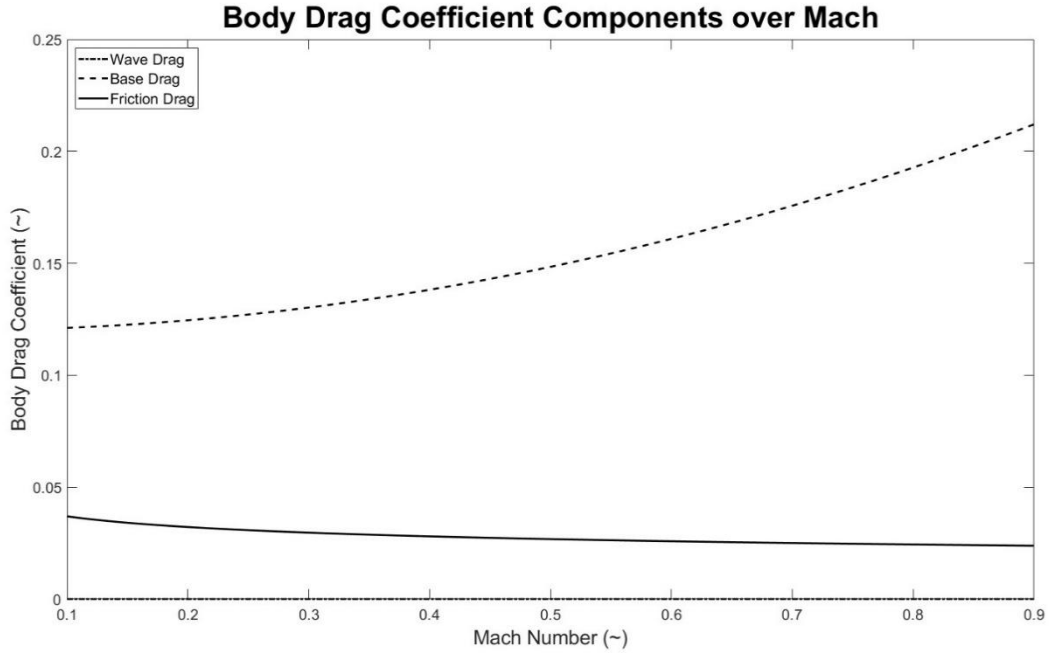

Figure 5 Components of Coast Drag for Mach Range

For the given Mach range, base drag is the dominant contributor towards the drag coefficient. Wave drag is seen as zero, and skin friction is less than base drag, but still significant. The main variables that support the base drag are the Mach number, while the skin friction is mostly a function of the body fineness ratio, which for the JASSM is 0.133. Since Mach number only reduces the skin friction, the coefficient can only be less than the fineness ratio, which is less than the base drag for most Mach numbers.

B. Body Normal Force

In Table 2 and Figure 6 an evaluation of the body only aerodynamic efficiency is conducted to the base line model. The body lift to drag ratio (L/D) is calculated as a function of angle of attack α for roll angles $\phi = 0{,}30{,}45\ deg$. The analysis isolated the missile fuselage without wings or tail as a benchmark for comparison.

Table 2 Body L/D over different angle of attack and roll angle

$\phi\ (deg)$	$\left(\frac{L}{D}\right)_{max}$
0	2.019
30	2.100
45	2.177

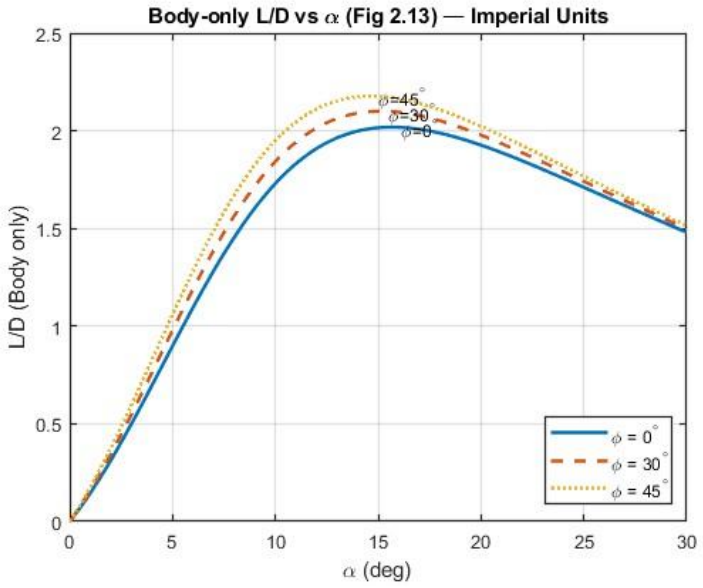

Figure 6 Body L/D over different angles of attack and roll angles

From Table 2 and Figure 6, the body L/D ratio grows with the increase of α antil the range of 5.4 - 5.8 deg. After this point, the drag increases more rapidly than lift leading to a decline in the L/D ratio. On the other hand the effect of roll angle is consistent on the body as larger roll angles lead to better L/D ratios and lower α . This effect is explained mathematically by the following equation showing the increase in as the roll angles increases.

$$G(\phi) = \left(\frac{a}{b}\right)\cos^2\phi + \left(\frac{b}{a}\right)\sin^2\phi \quad (5)$$

The missile body alone achieve a L/D ratio of almost 6 at angle of attack near 5.4 and a roll angle of 45 deg. These results provide a base line of the body lift efficiency and highlight the importance of including a lifting surface to enhance the missile aerodynamic performance.

C. Mean Aerodynamic Center

Figure 7 illustrates the calculated position of the missile body's aerodynamic center $(x_{ac})_B$ as a function of the angle of attack α. The plot shows a clear trend where the aerodynamic center moves aft (rearward) as the angle of attack increases from 0º to 90º. At an angle of attack of 0º, the aerodynamic center is at its most forward position, (xac)B / ln = 0.63. As α increases, the location shifts rearward along a sinusoidal curve, reaching its maximum aft position of (xac)B / ln = 1.77 at an angle of attack of 90 deg.

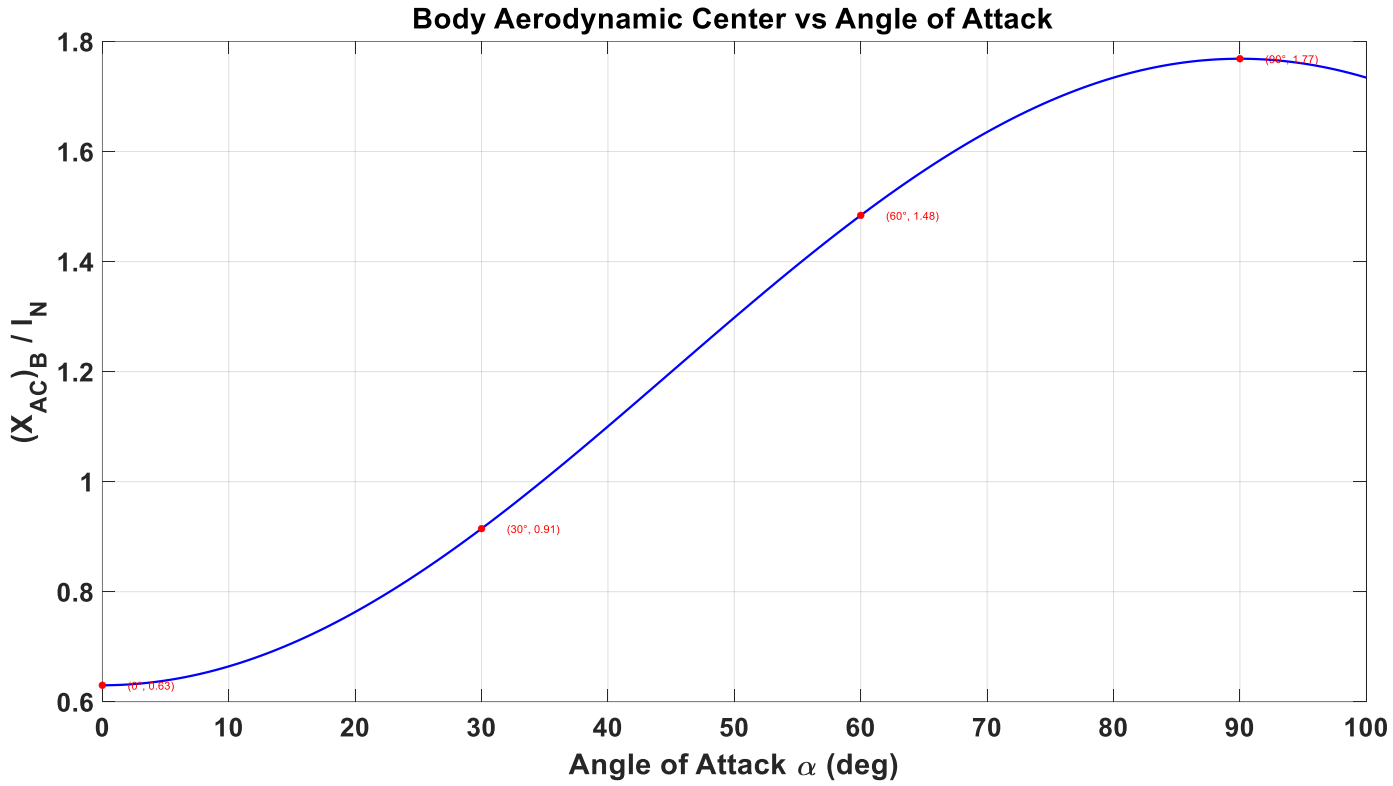

Figure 7 Body Aerodynamic Center vs Angle of Attack

V. Missile Planar Surfaces and Aerodynamic Center

D. Planar Geometry

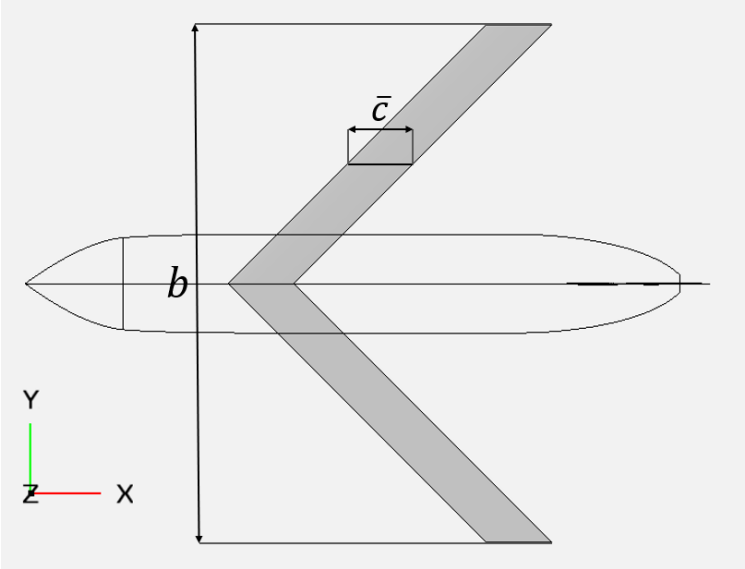

Figure 8 OpenVSP Missile Wing Geometry [7]

Using reference images and having a known wingspan of 7.87 feet, the remaining geometry could be determined. The measured geometry is shown in the table below.

Table 3 Measured Planar Geometry

Wingspan (b)	Root Chord (c_r)	Tip Chord (c_t)	Leading Edge Sweep (Λ_{LE})
7.87 ft	1.00 ft	1.00 ft	45 degrees

Calculating the remaining geometry using this set of equations:

$$\lambda = \frac{c_t}{c_r} \tag{6}$$

$$S = \frac{b}{2} c_r (1 + \lambda) \tag{7}$$

$$\bar{c} = \frac{2}{3} c_r \frac{1+\lambda+\lambda^2}{1+\lambda} \tag{8}$$

The result of which are displayed in the table below:

Table 4 Calculated Planar Geometry

Taper ratio (λ)	Wing Area (S)	Mean Aerodynamic Chord ($\bar{c}$)
1.0	7.87 ft^2	1.0 ft

E. Planar Normal Force

The planar normal forces for the JASSM configuration were evaluated using lifting surface theory, which provides an appropriate approximation for subsonic flight regimes and high-aspect-ratio

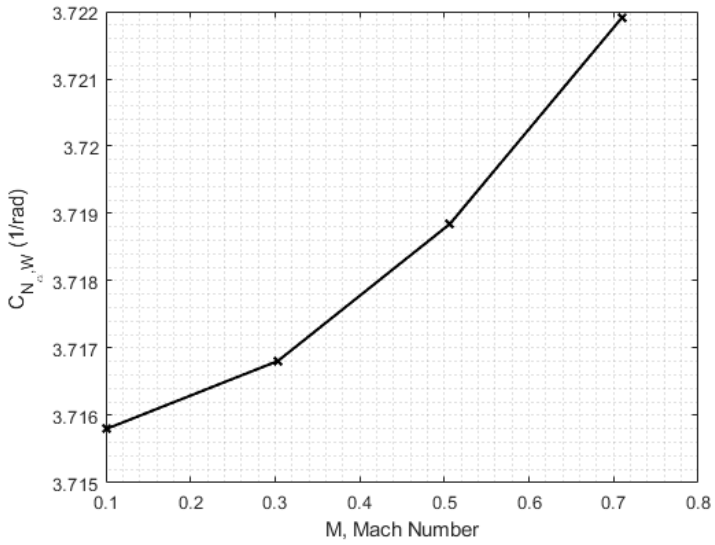

Figure 9 C_{N_α} through Flight Envelope

lifting surfaces. Since the JASSM wing has a relatively large aspect ratio, the flow can be reasonably modeled under the assumptions of linear lifting surface theory, which accounts for the spanwise variation in circulation and the finite-wing correction to lift slope. In this formulation, the coefficient of normal force with respect to angle of attack, C_{N_α}, is directly related to the classical lift curve slope, C_{L_α}, derived from thin airfoil theory and corrected for finite aspect ratio effects. By invoking small-angle approximations, it follows that $C_{L_\alpha} \approx C_{N_\alpha}$, enabling the normal force coefficient to be expressed as a linear function of the angle of attack. This relationship is particularly valid in the low-angle regime relevant to the JASSM mission profile. For the planform analysis, the effective angle of attack is assumed to remain below 10 degrees, ensuring that the flow remains attached and that nonlinear aerodynamic effects such as stall or vortex lift do not dominate. The use of this theory is consistent with standard missile aerodynamics practice, where slender body contributions are considered separately, and planar surface contributions can be treated using classical lifting-line and lifting-surface methods.

$$(C_{N_\alpha})_{\text{surface}} = \frac{dC_N}{d\alpha} \approx \frac{dC_L}{d\alpha} = \frac{2\pi A}{2+\sqrt{A^2\left(1+\tan^2\Lambda_{LE}\right)-M^2+4}} \quad [\text{rad}^{-1}] \quad [8] \tag{9}$$

The normal force characteristics were evaluated by plotting the coefficient of normal force with respect to angle of attack, C_{n_α}, across the Mach number range of interest, and subsequently calculating the corresponding values using the governing equations shown below. It should be noted that the dependence of C_{n_α} on Mach number in the subsonic regime is relatively weak; the coefficient exhibits only minor variation as compressibility effects remain limited at the operating flight conditions of the JASSM. This observation allows for the assumption that the normal force slope remains nearly constant throughout subsonic cruise, provided that the angle of attack remains within the small-angle approximation.

$$(C_{N_\alpha})_{Tot} = (C_{N_\alpha})_W (S_W / S_{ref}) + (C_{N_\alpha})_B \tag{10}$$

After determining the normal force slope, C_{n_α}, the total normal force coefficient for the complete missile configuration can be expressed as a function of angle of attack. By applying the linear relation between normal force and angle of attack within the small-angle regime, the aggregate normal force coefficient, C_n, is obtained by summing the contributions from all relevant lifting surfaces, including the wing, tail, and body effects. This formulation allows the overall aerodynamic response of the missile to be represented as:

$$C_N = C_{N_\alpha} \alpha \tag{11}$$

where α is the effective angle of attack in radians. It is assumed that the normal force equals zero at a zero angle of attack.

$$C_N = (C_N)_W + (C_N)_B \tag{12}$$

Plotting C_n across a range of angles of attack provides a direct visualization characteristics in the subsonic flight envelope. The slope of this curve indicates the sensitivity of the total normal force to small perturbations in angles of attack, which is essential in predicting static stability margins and assessing the linear aerodynamic behavior prior to the onset of nonlinear effects such as flow separation or stall.

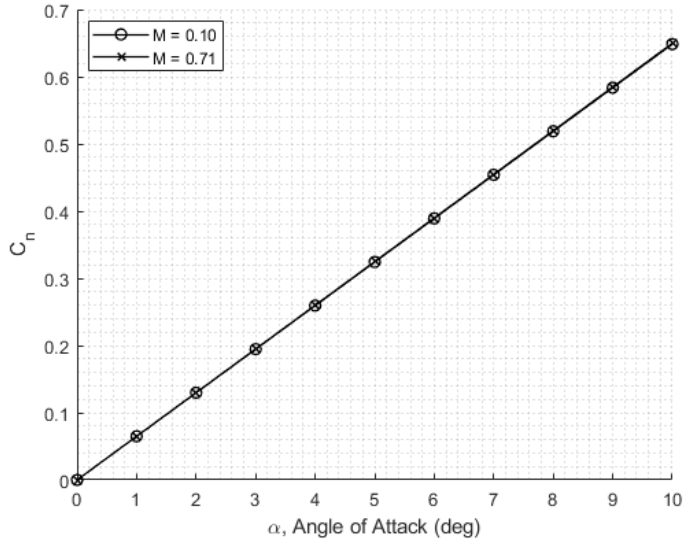

Figure 10 $(C_N)_W$ over Angles of Attack

Adding both C_{N_α} terms and C_N terms for the missile body and the wing, using the equations stated previously, the following figures are produced. These shows the total missile C_{N_α} over the flight regime and the total C_N over angles of attack.

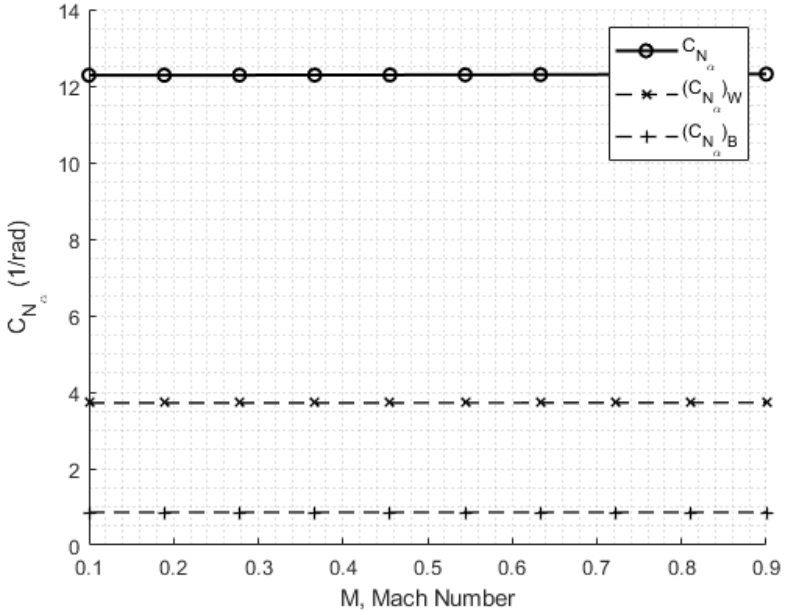

Figure 11 Total C_{N_α} over Flight Envelope

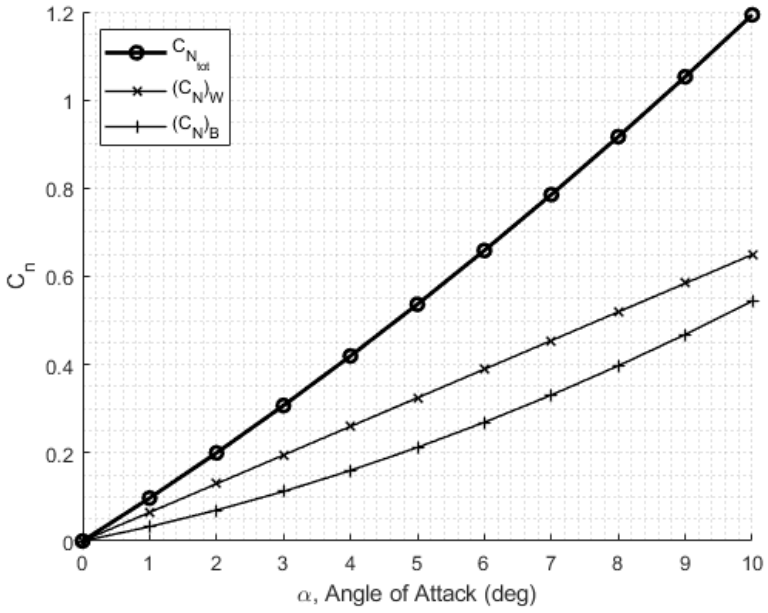

Figure 12 Total C_N over Angles of Attack

F. Planar Drag Force

Since the JASSM operates entirely within the subsonic flight regime, the primary drag contribution attributed to the planar surfaces is due to viscous skin friction. By evaluating the surface friction drag across the relevant Mach numbers, the distribution of frictional drag is obtained and is presented in Figure #. This trend directly reflects the influence of Reynolds number variation with Mach number, as increasing dynamic pressure reduces the relative boundary-layer thickness and alters the local skin friction coefficient.

$$\left(C_{D_0}\right)_{\text{Surface,Friction}} = n_{\text{surface}}\left[0.0133\left(\frac{M}{qc_{\text{mac}}}\right)^{0.2}\right]\left(\frac{2S_{\text{surface}}}{S_{\text{ref}}}\right) \tag{13}$$

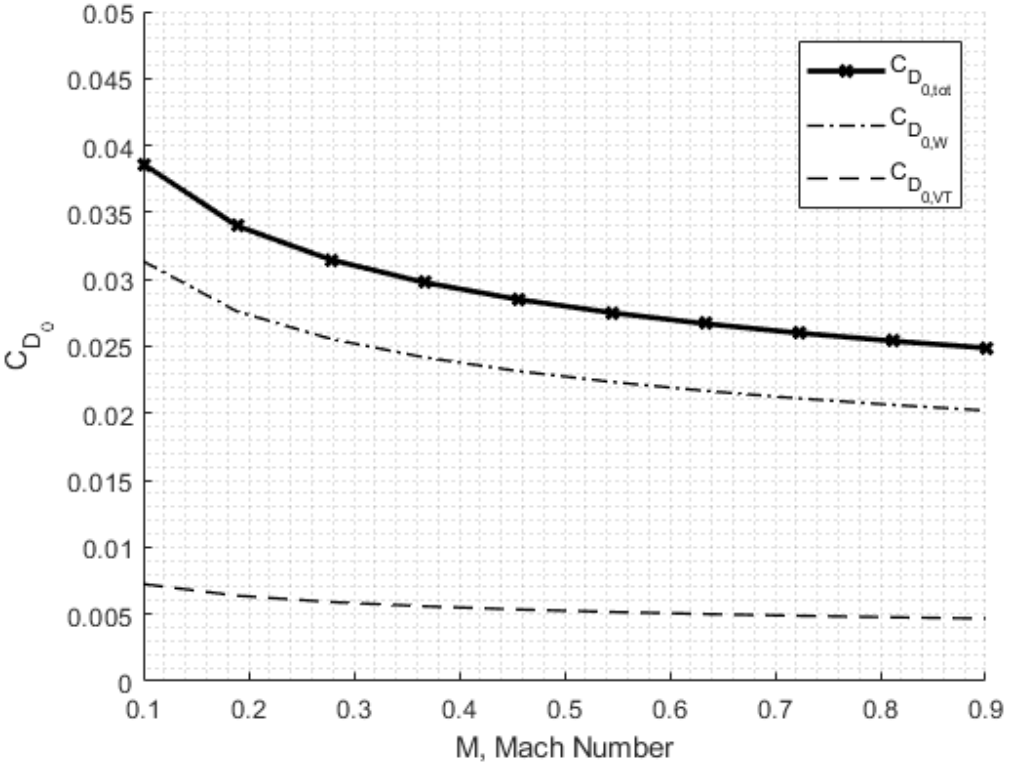

Figure 13 Friction Drag through Flight Envelope

G. Planar Aerodynamic Center

The aerodynamic center of the wing shifts due to changes in Mach number in flight.

$$\left(\frac{x_{AC}}{c_{mac}}\right)_{Surface} = \frac{A(M^2-1)^{\frac{1}{2}}-0.67}{2A(M^2-1)^{\frac{1}{2}}-1}, \text{ if } M > 2.0 \tag{14}$$

$$\left(\frac{x_{AC}}{c_{mac}}\right)_{Surface} = 0.25, \text{ if } M < 0.7 \tag{15}$$

The region between M = 0.7 – 2.0 is assumed to be linear, this is done to simplify the transonic region. Applying these equations to the wing results in a constant, linear plot over our flight envelope. Since the location does not change below M = 0.7. This is shown in ##.

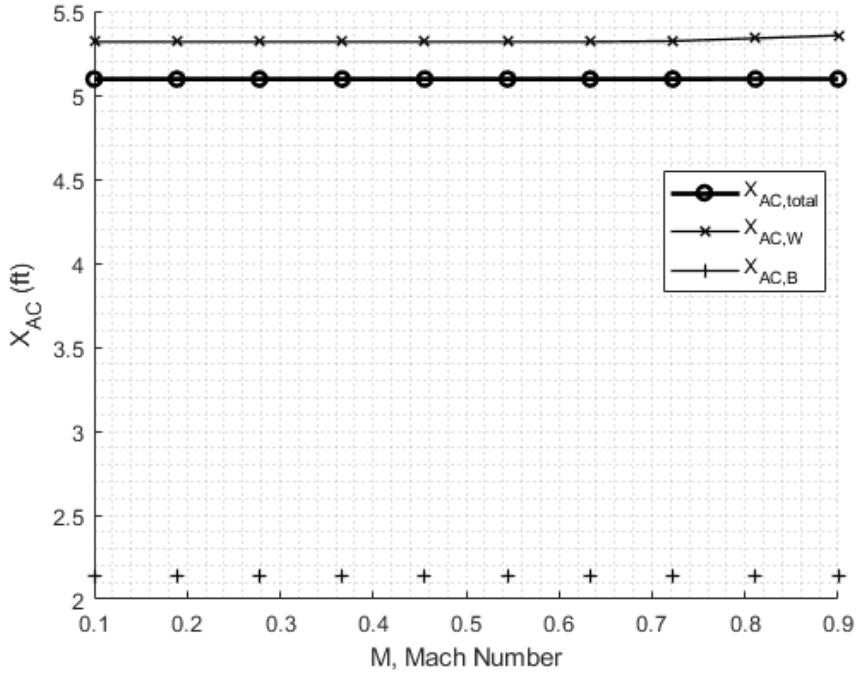

Figure 14 Aerodynamic Center Over Flight Envelope

VI. Cruise Flight

Cruise conditions:
Altitude: 10,000 ft
Mach Number: 0.71
Cruise AoA: $\alpha \leq 10$

The cruise performance test for the missile was conducted to determine if the body and wing configuration can sustain a steady level flight at a. lower altitude. In this analysis we assumed a 10,000 feet altitude with a Mach number of 0.71 representing a subsonic long-range cruise. For this missile the design constraint is that at an $\alpha < 10$ The lift generated by the missile must equal the weight of the missile. Normal force coefficient and drag coefficient were calculated in previous sections and used here.

To calculate the lift coefficient both normal and drag coefficient were used in the following formula.

$$C_L(\alpha) = C_N(\alpha)cos\alpha - C_{D0,tot}sin\alpha \quad (16)$$

The dynamic pressure at 10,000 ft and Mach 0.71 is calculated in standard atmosphere and used to calculate the lift in the following equation.

$$L(\alpha) = C_L(\alpha)qS_{ref} \quad (17)$$

Table 5 cruise condition and results

Parameter	**Values**
Altitude	10,000 ft
Mach number	0.71
Dynamic pressure	23,900 Pa
Weight (W)	2,250 lbf
Reference area (S_{ref})	2.56 ft^2
Wing area (S_{Wing})	7.78ft^2
Cruise satisfied at α	5.8 Deg

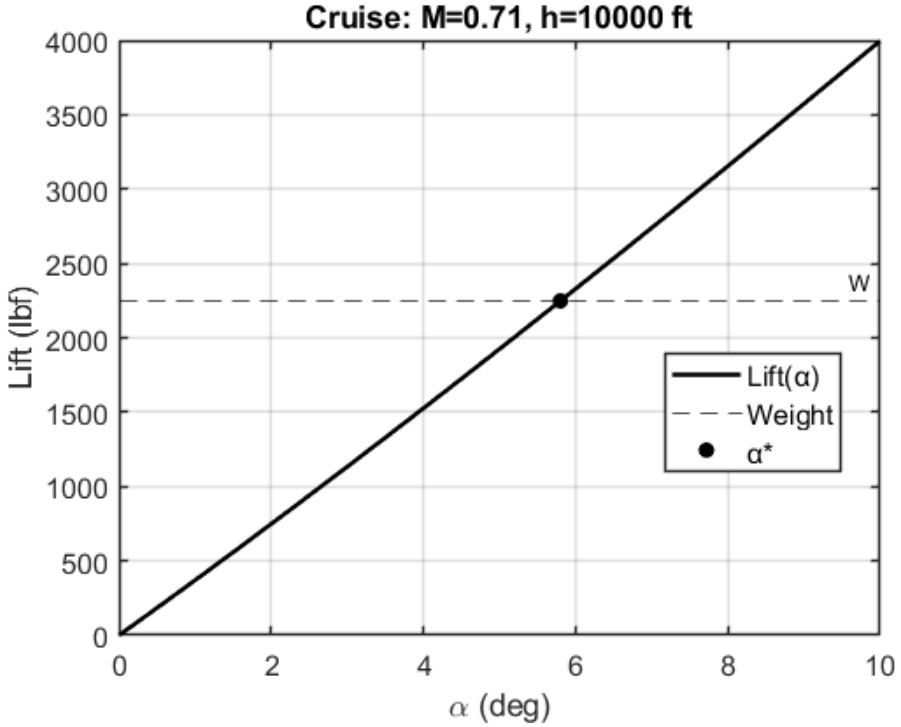

Figure 15 Cruise Lift per Angle of Attack

From Table 5 and Figure 15 the missile body and wing surface satisfies the required cruise conditions at an angle of attack of $\alpha = 5.8$ as that the missile will generate lift equal to the weight at that angle. Within $\alpha < 10°$ the maximum lift generated 4,000 lbf almost twice the weight indicating that the missile design has sufficient lift generated.

The angle of attack at which the cruise is achieved shows that the chosen wing geometry is adequate for a Mack 0.71 cruise in a lower atmosphere. The fuselage does generate lift, but the addition of lifting surface is required to reduce the α into a practical operating range.

VII. Tail Sizing and Control Surface

H. Tail Surface Area

To justify treating the missile as a tailless configuration, the required horizontal tail area was evaluated from stability relations based on the wing and body contributions. The equation for tailing sizing is shown below.

$$\frac{S_T}{S_{\text{Ref}}} = (C_{N_\alpha})_B \frac{x_{CG} - (x_{AC})_B}{d} + (C_{N_\alpha})_W \frac{x_{CG} - (x_{AC})_W}{d} \left(\frac{S_W}{S_{\text{Ref}}} \right) + \frac{\left[(C_{N_\alpha})_B + (C_{N_\alpha})_W \frac{S_W}{S_{\text{Ref}}} \right] \frac{x_{AC} - x_{CG}}{d}}{(C_{N_\alpha})_T \frac{(x_{AC})_T - x_{CG}}{d} - \frac{x_{AC} - x_{CG}}{d}} \tag{18}$$

Rearranging the equation to solve for a static margin equal to zero results in the equation below.

$$S_T = \left\{ (C_{N_\alpha})_B \frac{x_{CG} - (x_{AC})_B}{d} + (C_{N_\alpha})_W \frac{x_{CG} - (x_{AC})_W}{d} \left(\frac{S_W}{S_{\text{Ref}}} \right) \right\} \left(\frac{d}{(x_{AC})_T - x_{CG}} \right) \frac{S_{\text{Ref}}}{(C_{N_\alpha})_T} \tag{19}$$

By having an undetermined x_{CG}, and all other variables determined, the required tail area could be determined using the equation above. The results show that the wing-body system alone provides sufficient stability margin, and no additional horizontal tail surface area is required. Plotting S_T / S_{Ref} through a range of Mach numbers of results in the figure below. In subsonic flight, the required tail area remains constant, shown in the figure below. Moving to the location shown in the graph below results in a tail area of zero. The location shown in the figure below is measured from the nose of the missile.

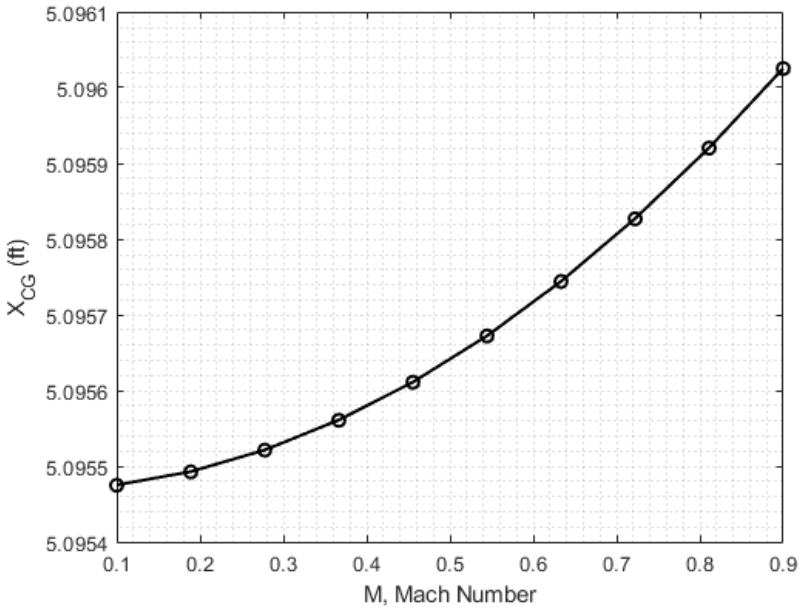

Figure 16 C.G. Location for Zero Tail Area

Using slender wing theory and using an example tail using the missile geometry as a base. The tail geometry from the figure below was used to find the tail normal force.

Figure 17 OpenVSP Example Tail Geometry [7]

The tail normal force was calculated using slender wing theory, shown the equations below. Using the figure above the Aspect Ratio (A_T), was determined to be 0.628. Checking using the equations below confirms that slender wing theory can be used for this application.

$$(C_{N_\alpha}) = \pi A_T / 2, \quad M < [1 + [8/(\pi A)^2]]^{1/2} \tag{20}$$

For $A = 0.628$, M < 1.7479

Using this, the $(C_{N_\alpha})_T$ was determined to be 0.9865 rad^{-1}, with x_{AC_T} located at 8.0975 ft from the missile nose. Implementing these into the previous equations results in a tail sizing plot for the JASSM at three different C.G. locations. With small changes in C.G. location, large tail sizes are required to compensate. The figure shows that the sizing remains constant throughout the missile's flight.

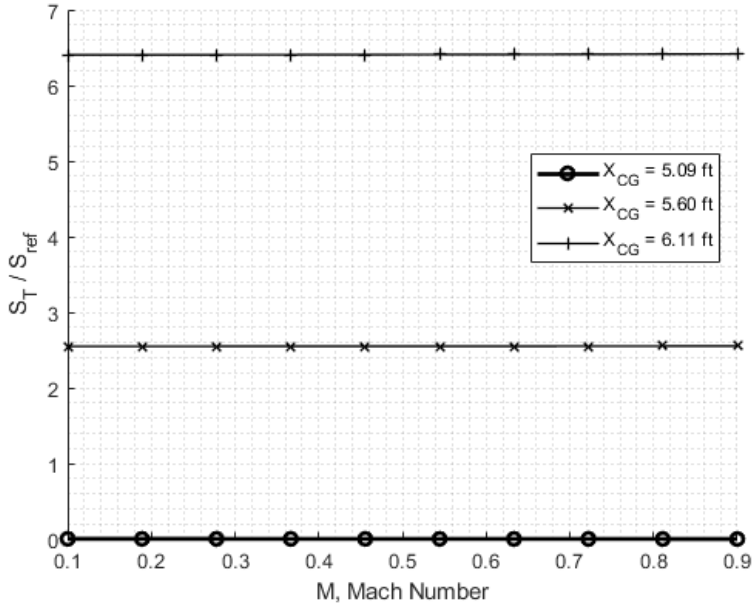

Figure 18 Tail Area Ratio Over Flight Envelope for Varying C.G. locations

I. Wing Hinge Moment

The wing hinge moment is described as:

$$HM_{wing} = N_{wing}\left(\frac{X_{AC} - X_{HL}}{\bar{c}}\right)_{wing} \tag{21}$$

where N_{Wing} is the wing planar normal force, X_{AC} is the aerodynamic-center location, X_{HL} is the hinge-line location, and $\bar{c}$ is the mean aerodynamic chord from the wing. For this analysis the hinge line is fixed at $0.75\ \bar{c}$ from the leading edge, and the aerodynamic center is held at $0.25\ \bar{c}$ from the leading edge across the flight envelope. Geometry of the hinge moment is shown in Figure 19 below.

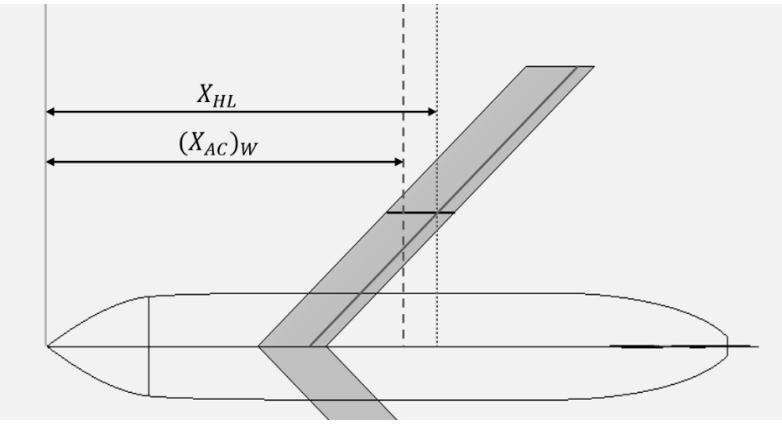

Figure 19 Wing Hinge Moment Geometry

Plotting the hinge moment through effective angles of attack results in Figure 20. The hinge moment slope increases with an increase in dynamic pressure, making the hinge moments diverge significantly at higher angles of attack.

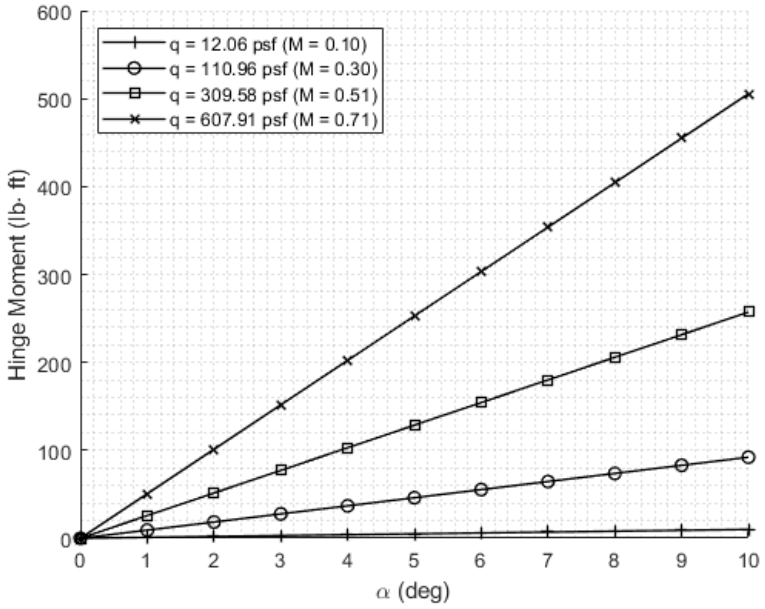

Figure 20 Hinge Moment through Effective Angles of Attack

VIII. References

[1] Svitlyk, Y. "AGM-158 JASSM: Joint Air-to-Surface Standoff Missile." Root Nation, November 25, 2024. https://root-nation.com/en/articles-en/weapons-en/en-agm-158-jassm-air-launched-cruise-missile/

[2] Siemens Digital Industries Software, *NX* [computer software], Version 2306, Siemens Digital Industries Software, Plano, TX, 2023. URL: https://www.plm.automation.siemens.com/global/en/products/nx/

[3] USAF launches JASSM New Variant Missile. Default. (n.d.). https://www.janes.com/osint-insights/defence-news/weapons/usaf-launches-jassm-new-variant-missile

[4] UPDATED JASSM® completes important Lockheed martin flight tests. Media - Lockheed Martin. (n.d.). https://news.lockheedmartin.com/2017-03-08-Updated-JASSM-R-Completes-Important-Lockheed-Martin-Flight-Tests

[5] U.S. Standard Atmosphere, 1976, NOAA-S/T-76-1562, NASA-TM-X-74335, National Oceanic and Atmospheric Administration, Washington, D.C., Oct. 1976. Available: https://www.robertribando.com/xls/fluid-mechanics/1976-u-s-standard-atmosphere/

[6] Fleeman, E. L., & Schetz, J. A. (2012). *Missile Design and System Engineering*. American Institute of Aeronautics and Astronautics.

[7] OpenVSP, *Open Vehicle Sketch Pad (OpenVSP), Version 3.33.0*, NASA Open Source Software, 2025. Available: https://openvsp.org

[8] Drela, M. Flight Vehicle Aerodynamics. Cambridge, MA: MIT Press, 2014.

[9] The MathWorks Inc., *MATLAB, Version 9.15.0 (R2024b)*, Natick, MA, 2024. Available: https://www.mathworks.com

IX. Appendix A

The following is the complete code for this report, using MATLAB [9].

```
% Baseline Aerodynamics
clear; clc; close all

%% Geometry
% Body Geometry
% d (from body)
Sref = 2.56;

% Wing Geometry [ft, deg]
% Input Measured Geometry [b,cr,ct,LLe,XLE] ---> Output [S,A,mac,Xac]

            %   b,  cr,  ct, LLe, XLE
wing_meas = [7.87, 1.0, 1.0,   45, 3.1];
            %   b,  cr,  ct, LLe, XLE
vt_meas =   [1.3, 1.5, 1.3,   35, 8.25];

[Sw, Aw, mac_w, Xac_w, Svt, Avt, Xac_vt] = planform_from_meas(wing_meas, vt_meas);
XLE_mac = Xac_w - 0.25 * mac_w;


%% Standard Atmosphere
% Calculator for atmospheric states throughout entire and operational
% atmosphere, as well as dynamic pressure plots for operation Mach regime
% for different missions
% Written By Nathaniel Hollman

% Sea Level Conditions
state0 = [14.7, 518.67, 0.002377]; % [p, T, rho]
gas = [1.4, 1717.5, 0]; % [gamma (~), R lb/slugR, cp*]
a0 = (gas(1)*gas(2)*state0(2))^0.5;

% Entire Atmos Alt and Operational Alt
altp1 = 80000;
altp2 = 40000;

[a_av, alts_op, states_op] = atmos_plots(altp1, altp2, a0);

% OPERATIONAL & MISSION MACH, QBAR, & ALT DATA

% Predefines states for code efficiency
states_op1 = zeros([4, 3]);
states_op2 = zeros([4, 3]);

% Mission 1 - Dropped from C-130
% [Dropped from Crate, Begins Engine, Cruises, hits target]
Alts_op1 = [10000, 5000, 2000, 10]; % ft
Ms_op1 = [0.1, 0.3, 0.71, 0.9];
Vs_op1 = a_av*Ms_op1;
for i = 1:4
    states_op1(i,:) = Standard_Atmos(Alts_op1(i),'ft',state0);
```

```
end
qbar_op1 = 0.5*Vs_op1.^2.*states_op1(:,3)';

% Mission 2 - Launched from F-22
% [Dropped from Wing, Begins Engine, Cruises, hits target]
Alts_op2 = [40000, 30000, 2000, 10]; % ft
Ms_op2 = [0.9, 0.6, 0.71, 0.9];
Vs_op2 = a_av*Ms_op2;
for i = 1:4
    states_op2(i,:) = Standard_Atmos(Alts_op2(i),'ft',state0);
end
qbar_op2 = 0.5*Vs_op2.^2.*states_op2(:,3)';

% Operational Mach Range and Altitude Range Data
% Dynamic Pressure with Mach Speeds
Ms = linspace(0.1,0.9,10);
Vs = a_av*Ms;
dens_op = states_op(:,3)*state0(3);
qbar = 0.5*Vs.^2.*dens_op;

% QBAR, ALTITUDE, AND MACH PLOTS
qbar_Mach_Plot(Ms, qbar, alts_op, qbar_op1, Alts_op1, qbar_op2, Alts_op2)

%% Missile Body

% ===== 1) User Inputs =====
% Body geometry [ft]
a = 10.00/12;          % semi-major axis [ft]  (10 in)
b = 11.67/12;          % semi-minor axis [ft]  (11.67 in)
l = 161.95/12;         % body length [ft]      (161.95 in)
l_nt = 40.68/12;       % nose tip length [ft]  (40.68 in)
Ae = 23.76/144;        % effective area of exhaust [ft2] (23.76 in2)
d_eff    = 2*sqrt(a*b);               % effective diameter [ft]
LD_ratio = l/d_eff;                   % slenderness l/d_eff (dimensionless)

%% Body Drag
% Body Drag per Mach number for powered and unpowered flight

% Cruise Conditions

M_c = 0.71;
alt_c = 2000; % ft
states_c = Standard_Atmos(alt_c,'ft',state0); % States at Cruise Altitude
V_c = M_c*(gas(1)*gas(2)*states_c(2))^0.5; % cruise velocity (ft/s)

% JASSM Body Geometry for Functions
body_geo = [l, d_eff, l_nt, 0, a, b]; % [l, d, l_ns, d_nstp, a, b] (in)

% Body Drag per Mach number for powered cruise
C_D_Body = Body_Drag(gas, states_c, V_c, body_geo, Ae);
fprintf('The Cruise Flight Drag Coefficient is %0.4f ', C_D_Body)

% DRAG PLOTS CALCULATIONS
Drag_Plots(0.1, 0.9, gas, states_c, body_geo, Ae, a_av)
```

```
%% Body Lift
% Mohamed Almazrouei


alpha_deg    = linspace(0,30,301);
alpha        = deg2rad(alpha_deg);
phi_list_deg = [0, 30, 45];
phi_list     = deg2rad(phi_list_deg);


CD0_body = C_D_Body;

bodyCN = @(aa,phi) ...
    ((a/b)*cos(phi).^2 + (b/a)*sin(phi).^2) .* ...
    ( abs(sin(2*aa).*cos(aa/2)) + 1.3*LD_ratio.*(sin(aa).^2) );

% Lift-to-drag
LD_fun = @(aa,CN,CD0) ( CN.*cos(aa) - CD0.*sin(aa) ) ./ ...
                      ( CN.*sin(aa) + CD0.*cos(aa) );

% Compute and Plot
figure; hold on; grid on; box on;

lineStyles = {'-','--',':','-.'};

best_alpha = zeros(1,numel(phi_list));
best_LD    = zeros(1,numel(phi_list));

for i = 1:numel(phi_list)
    phi = phi_list(i);
    CN  = bodyCN(alpha, phi);
    LD  = LD_fun(alpha, CN, CD0_body);

    [LDmax, idx] = max(LD);
    best_LD(i)    = LDmax;
    best_alpha(i) = alpha_deg(idx);


    plot(alpha_deg, LD, ...
        'LineWidth', 1.8, ...
        'LineStyle', lineStyles{mod(i-1,numel(lineStyles))+1}, ...
        'DisplayName', sprintf('\\phi = %d^\\circ', phi_list_deg(i)));

    text(best_alpha(i)+0.4, best_LD(i), ...
        sprintf('\\phi=%d^\\circ', phi_list_deg(i)), ...
        'FontSize', 9, 'Color', 'k');
end

xlabel('\alpha (deg)'); ylabel('L/D (Body only)');
title('Body-only L/D vs \alpha (Fig 2.13) — Imperial Units');
legend('Location','best','TextColor','k');
set(gca,'LineWidth',1);  % nicer for printing


fprintf('---- Body-only L/D (CD0_body=%.3f) ----\n', CD0_body);
```

```
fprintf(' phi [deg] | alpha* [deg] | (L/D)_max\n');
fprintf('-------------------------------------\n');
for i = 1:numel(phi_list_deg)
    fprintf('   %2d      |   %6.2f     |   %6.3f\n', ...
        phi_list_deg(i), best_alpha(i), best_LD(i));
end

[~, ig] = max(best_LD);
fprintf('\nWrite-up:\n');
fprintf(['Body-only L/D grows with \\alpha up to an optimum near \\alpha* = %.2f deg
' ...
         '(for \\phi = %d^\\circ). Increasing roll angle modifies the geometric
factor ' ...
         'G(\\phi)=(a/b)cos^2\\phi+(b/a)sin^2\\phi, shifting CN and therefore the
peak L/D ' ...
         'and the corresponding \\alpha*.\n'], best_alpha(ig), phi_list_deg(ig));

%% Mean Aerodynamic Center
% BODY AERODYNAMIC Center VS ANGLE OF ATTACK PLOT
% Tri Phan
% Geometry
lB = 143.9;    % Body length (in)
lN = 40.68;    % Nose length (in)
lB_lN = lB / lN;   % Body-to-nose length ratio

% Angle of attack range (degrees)
alpha = linspace(0, 100, 500);
alpha_rad = deg2rad(alpha);

% Equation:
% (Xac)_B / lN = 0.63*(1 - sin^2(alpha)) + 0.5*(lB/lN)*sin^2(alpha)
Xac_lN = 0.63*(cos(alpha_rad).^2) + 0.5*lB_lN.*(sin(alpha_rad).^2);

% ---- Plot ----
figure;
plot(alpha, Xac_lN, 'b-', 'LineWidth', 2); hold on; grid on;

% Add markers at key points
alpha_points = [0 30 60 90];
alpha_rad_points = deg2rad(alpha_points);
Xac_points = 0.63*(cos(alpha_rad_points).^2) + 0.5*lB_lN.*(sin(alpha_rad_points).^2);

plot(alpha_points, Xac_points, 'ro', 'MarkerFaceColor', 'r');

% Annotate values
for i = 1:length(alpha_points)
    text(alpha_points(i)+2, Xac_points(i), ...
        sprintf('(%d°, %.2f)', alpha_points(i), Xac_points(i)), ...
        'FontSize', 10, 'Color', 'r');
end

xlabel('Angle of Attack \alpha (deg)', 'FontSize', 12);
ylabel('(X_{AC})_B / l_N', 'FontSize', 12);
title('Body Aerodynamic Center vs Angle of Attack', 'FontSize', 13);
xlim([0 100]);
```

```
%% Missile Planar Surfaces
% Tiger Sievers

% ------------------------------
% Wing normal-force slope vs Mach (body-ref)
% CN_alpha_wing = f(M, A, LLE)
% ------------------------------
M_sweep = Ms;
q_sweep = 0.5 .* states_c(3) * (M_sweep * a_av).^2;
LLe_w = wing_meas(4);                  % deg
CN_alpha_wing = PlanNorm(Aw, LLe_w, M_sweep);   % 1/rad, referenced to Sref (assumed)
CN_alpha_body(1:numel(Ms)) = 2.*(a./b)*cos(phi).^2; % 1/rad assuming no roll, phi =
0;

% Adding Together
CNa_Tot = CN_alpha_wing * (Sw./Sref) + CN_alpha_body;

% Plot CNa_w(M)
figure
hold on
plot(M_sweep, CNa_Tot, 'LineWidth',1.5, 'Color','k', 'Marker','o')
plot(M_sweep, CN_alpha_wing, 'LineWidth',1, 'Color','k', 'Marker','x','LineStyle','--
')
plot(M_sweep, CN_alpha_body, 'LineWidth',1, 'Color','k', 'Marker','+','LineStyle','--
')
legend('C_{N_\alpha}','(C_{N_\alpha})_W','(C_{N_\alpha})_B')
grid minor
xlabel('M, Mach Number'); ylabel('C_{N_\alpha} (1/rad)')

% ------------------------------
% AoA sweep at two Mach points
% ------------------------------
alpha_sweep = 0:1:10;                  % deg
alpha_rad   = deg2rad(alpha_sweep(:)); % Nx1
CN_wing_lo  = CN_alpha_wing(1)  .* alpha_rad;
CN_wing_hi  = CN_alpha_wing(end).* alpha_rad;

figure; hold on
plot(alpha_sweep, CN_wing_lo, 'Color','k', 'LineWidth',1, 'Marker','o')
plot(alpha_sweep, CN_wing_hi, 'Color','k', 'LineWidth',1, 'Marker','x')
grid minor
xlabel('\alpha, Angle of Attack (deg)'); ylabel('C_n')
legend(sprintf('M = %.2f', M_sweep(1)), sprintf('M = %.2f', M_sweep(end)),
'Location','best')

% ------------------------------
% AoA sweep at cruise Mach point
% ------------------------------
CN_wing_c  = CN_alpha_wing(7).* alpha_rad;
CN = CN_wing_c + bodyCN(alpha_rad, 0);

figure; hold on
plot(alpha_sweep, CN, 'Color','k', 'LineWidth',2, 'Marker','o')
plot(alpha_sweep, CN_wing_c, 'Color','k', 'LineWidth',1, 'Marker','x')
```

```
plot(alpha_sweep, bodyCN(alpha_rad, 0), 'Color','k', 'LineWidth',1, 'Marker','+')
grid minor
xlabel('\alpha, Angle of Attack (deg)'); ylabel('C_n')
legend('C_{N_{tot}}', '(C_{N})_W','(C_{N})_B' ,'Location','northwest')

% ------------------------------
% Planar friction drag (no wave)
% PlanFrict(M, q, n_panels, mac, S, Sref) -> CD0 of that surface
% ------------------------------
n_w  = 1;
CD0_wf  = PlanFrict(M_sweep, q_sweep, n_w, mac_w, Sw,  Sref);

n_vt = 1;
% Use a characteristic length for the VT. If you don't have mac_vt, reuse mac_w.
CD0_vtf = PlanFrict(M_sweep, q_sweep, n_vt, mac_w, Svt, Sref);

CD0 = CD0_wf + CD0_vtf;

figure; hold on
plot(M_sweep, CD0,    'k', 'LineWidth',2, 'Marker','x')
plot(M_sweep, CD0_wf, 'k', 'LineWidth',1, 'LineStyle','-.')
plot(M_sweep, CD0_vtf,'k', 'LineWidth',1, 'LineStyle','--')
grid minor
xlabel('M, Mach Number'); ylabel('C_{D_0}')
ylim([0, 0.05])
legend('C_{D_{0,tot}}', 'C_{D_{0,W}}', 'C_{D_{0,VT}}', 'Location','best')

% ------------------------------
% Aerodynamic center (body + wing)
% Need CNaB(M) and xacB (ft), both body-referenced
% ------------------------------
% Convert lN from in --> ft and pick body AC at a baseline alpha
lN_ft = lN / 12;
xacB  = Xac_lN(1) * lN_ft;    % (Xac)_B at alpha = alpha(1)

% Wing AC shift with Mach (if your ac_update provides it)
% ac_update(M, A, mac, x_LE_mac, x_ac_ref) -> [Xac_old_out, Xac_wing(M)]
[Xac_old_out, Xac_wing] = ac_update(M_sweep, Aw, mac_w, (Xac_w - 0.25*mac_w), Xac_w);

% Combined AC (uses body-ref Sref)
% AeroCenter(CNaB, CNaW, Sw, Sref, xacB, xacW) -> XAC(M)
XAC = AeroCenter(CN_alpha_body, CN_alpha_wing, Sw, Sref, xacB, Xac_w);

figure
hold on
plot(M_sweep, XAC,       'k', 'LineWidth',2,'Marker','o')
plot(M_sweep, Xac_wing,  'k', 'LineWidth',1,'Marker','x')
plot(M_sweep, xacB,'k', 'LineWidth',1,'Marker','+')
grid minor
xlabel('M, Mach Number'); ylabel('X_{AC} (ft)')
legend('X_{AC,total}', 'X_{AC,W}', 'X_{AC,B}', 'Location','best')


%% Cruise Flight
% Mohamed Almazrouei
```

```
M_c   = 0.71;
alt_c = 10000;                                          % ft

% Atmosphere
states_c = Standard_Atmos(alt_c,'ft',state0);
T_abs = states_c(2) * state0(2);                        % Rankine
rho   = states_c(3) * state0(3);                        % slug/ft^3
a_c   = sqrt(gas(1) * gas(2) * T_abs);                  % ft/s
V_c   = M_c * a_c;                                      % ft/s
q_c   = 0.5 * rho * V_c^2;                              % psf


M_sweep = Ms;
q_sweep_cruise = 0.5 * rho * (M_sweep .* a_c).^2;   % psf vs Mach @ 10k ft

% AoA range
alpha_deg_cruise = 0:0.1:10;
alpha_cruise     = deg2rad(alpha_deg_cruise);
phi_cruise       = 0;
if ~exist('W','var') || isempty(W)
    W = 2250;                                           % lbf
end
tol_frac = 0.035;  tol_abs = tol_frac * W;

[~, iM_c] = min(abs(M_sweep - M_c));

%  CN
CN_body = bodyCN(alpha_cruise, phi_cruise);
CNaW_c  = CN_alpha_wing(iM_c);
CN_wing = (Sw/Sref) * (CNaW_c .* alpha_cruise);
CN_tot  = CN_body + CN_wing;

%  CD0 total
CD0_tot = C_D_Body + CD0_wf(iM_c) + CD0_vtf(iM_c);

%  CL and Lift
CL   = CN_tot .* cos(alpha_cruise) - CD0_tot .* sin(alpha_cruise);
Lift = CL .* q_c .* Sref;
CL_req = W / (q_c * Sref);


[err_min, kbest] = min(abs(Lift - W));
alpha_star = alpha_deg_cruise(kbest);
CL_star    = CL(kbest);
Lift_star  = Lift(kbest);
pass_ok    = err_min <= tol_abs;



%  Lift vs alpha
figure; hold on; grid on; box on
plot(alpha_deg_cruise, Lift, 'k', 'LineWidth', 1.8, 'DisplayName','Lift(α)')
yline(W, '--k', 'W', 'DisplayName','Weight')
plot(alpha_star, Lift_star, 'ko', 'MarkerFaceColor','k', 'DisplayName','α*')
```

```
xlabel('\alpha (deg)', 'FontSize', 14);
ylabel('Lift (lbf)', 'FontSize', 14);
title(sprintf('Cruise: M=%.2f, h=%.0f ft', M_c, alt_c), 'FontSize', 16);
legend('Location','best','FontSize',12);
set(gca,'FontSize',12,'LineWidth',1.2);


%% Tail Sizing
% ------------------------------
% Hinge moment (pick a Mach for the alpha sweep)
% HM = N_surf * (X_ac - X_hl);  N_surf = Cn * q * Sref   (body-ref)
% ------------------------------
Cn_alpha_sel = CN_alpha_wing;            % 1/rad
Cn_wing_sweep = Cn_alpha_sel .* alpha_rad;      % small-angle

Nw = Cn_wing_sweep .* q_sweep .* Sref;            % force [lb]
Xacw = Xac_w;                                   % ft
Xhl  = Xacw + 0.5*1.0;                          % ft (0.5 ft aft of AC)
HMw  = hinge_moment(Nw, Xacw, Xhl, mac_w);             % [lb*ft]

figure
hold on
plot(alpha_sweep, HMw(:,1), 'k', 'LineWidth',1.0, 'Marker','+')
plot(alpha_sweep, HMw(:,2), 'k', 'LineWidth',1.0, 'Marker','o')
plot(alpha_sweep, HMw(:,3), 'k', 'LineWidth',1.0, 'Marker','square')
plot(alpha_sweep, HMw(:,4), 'k', 'LineWidth',1.0, 'Marker','x')
legend('q = 12.06 psf (M = 0.10)', 'q = 110.96 psf (M = 0.30)', 'q = 309.58 psf (M =
0.51)', 'q = 607.91 psf (M = 0.71)', 'Location','northwest')
grid minor
xlabel('\alpha (deg)'); ylabel('Hinge Moment (lb\cdot ft)')

% ------------------------------
% Tail sizing & CG sweep (tailless check)
% ------------------------------
CNaW = CN_alpha_wing;  % scalar for the chosen Mach

% Tail
At = 0.628;
CNaT     = pi*At / 2;
xacT     = 8.0975; % [ft]

% Find CG giving ST=0 for the chosen Mach
[xCG_star, ST_of_x] = cg_for_zero_ST( ...
    CN_alpha_body, CNaW, CNaT, ...
    xacB, Xac_w, xacT, ...
    Sw, Sref, sqrt(4*Sref/pi));

xCG = xCG_star(end) + xCG_star(end)*[0.0, 0.1, 0.2]';

ST_S = TailAreaRatio( ...
    CN_alpha_body, CNaW, CNaT, ...
    xacB, Xacw, xacT, ...
    Sw, Sref, xCG);

figure
```

```
plot(M_sweep, xCG_star,'Marker','o','LineWidth',1.5,'Color','k')
xlabel('M, Mach Number')
ylabel('X_{CG} (ft)')
grid minor


figure
hold on
plot(M_sweep, ST_S(1,:),'Marker','o','LineWidth',2,'Color','k')
plot(M_sweep, ST_S(2,:),'Marker','x','LineWidth',1,'Color','k')
plot(M_sweep, ST_S(3,:),'Marker','+','LineWidth',1,'Color','k')
xlabel('M, Mach Number')
ylabel('S_{T} / S_{ref}')
grid minor
legend('X_{CG} = 5.09 ft', 'X_{CG} = 5.60 ft', 'X_{CG} = 6.11 ft','Location','best')
ylim([0,7])

%
```

X. Appendix B

I. Executive Summary – Nathaniel Hollman, Tiger Sievers, Tri Phan
II. Background – Tri Phan, Nathaniel Hollman, Tiger Sievers
    a. Mission Description – Nathaniel Hollman, Tri Phan
III. Standard Atmosphere – Nathaniel Hollman
IV. Missile Body – Tri Phan
    a. Body Drag – Nathaniel Hollman
    b. Body Normal Force – Mohamed Almazrouei
    c. Mean Aerodynamic Center – Tri Phan
V. Missile Planar Surfaces and Aerodynamic Center – Tiger Sievers
    a. Planar Geometry – Tiger Sievers
    b. Planar Normal Force – Tiger Sievers
    c. Planar Drag Force – Tiger Sievers
    d. Planar Aerodynamic Center – Tiger Sievers
VI. Cruise Flight – Mohamed Almazrouei
VII. Tail Sizing and Control Surface – Tiger Sievers
    a. Tail Surface Area – Tiger Sievers
    b. Wing Hinge Moment – Tiger Sievers